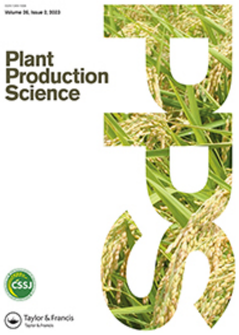

Plant Production Science

ISSN: (Print) (Online) Journal homepage: https://www.tandfonline.com/loi/tpps20

Biomass estimation of World rice (*Oryza sativa* L.) core collection based on the convolutional neural network and digital images of canopy

Kota Nakajima, Yu Tanaka, Keisuke Katsura, Tomoaki Yamaguchi, Tomoya Watanabe & Tatsuhiko Shiraiwa

To cite this article: Kota Nakajima, Yu Tanaka, Keisuke Katsura, Tomoaki Yamaguchi, Tomoya Watanabe & Tatsuhiko Shiraiwa (2023) Biomass estimation of World rice (*Oryza sativa* L.) core collection based on the convolutional neural network and digital images of canopy, Plant Production Science, 26:2, 187-196, DOI: 10.1080/1343943X.2023.2210767

To link to this article: https://doi.org/10.1080/1343943X.2023.2210767

PLANT PRODUCTION SCIENCE
2023, VOL. 26, NO. 2, 187–196
https://doi.org/10.1080/1343943X.2023.2210767

Taylor & Francis
Taylor & Francis Group

OPEN ACCESS Check for updates

Biomass estimation of World rice (*Oryza sativa* L.) core collection based on the convolutional neural network and digital images of canopy

Kota Nakajima[a], Yu Tanaka[b], Keisuke Katsura[c], Tomoaki Yamaguchi[c], Tomoya Watanabe[d] and Tatsuhiko Shiraiwa[a]

[a]Graduate School of Agriculture, Kyoto University, Kyoto, Japan; [b]Graduate School of Environmental, Life, Natural Science and Technology, Okayama University, Okayama, Japan; [c]United Graduate School of Agriculture Science, Tokyo University of Agriculture and Technology, Fuchu, Tokyo, Japan; [d]Independent researcher, Tokyo, Japan

ABSTRACT

Above-ground biomass (AGB) is an important indicator of crop productivity. Destructive measurements of AGB incur huge costs, and most non-destructive estimations cannot be applied to diverse cultivars having different canopy architectures. This insufficient access to AGB data has potentially limited improvements in crop productivity. Recently, a deep learning technique called convolutional neural network (CNN) has been applied to estimate crop AGB due to its high capacity for digital image recognition. However, the versatility of the CNN-based AGB estimation for diverse cultivars is still unclear. We established and evaluated a CNN-based estimation method for rice AGB using digital images with 59 diverse cultivars which were mostly in World Rice Core Collection. Across two years at two locations, we took 12,183 images of 59 cultivars with commercial digital cameras and manually obtained their corresponding AGB. The CNN model was established by using 28 cultivars and showed high accuracy ($R^2 = 0.95$) to the test dataset. We further evaluated the performance of the CNN model by using 31 cultivars, which were not in the model establishment. The CNN model successfully estimated AGB when the observed AGB was lesser than 924 g m^{-2} ($R^2 = 0.87$), whereas it underestimated AGB when the observed AGB was greater than 924 g m^{-2} ($R^2 = 0.02$). This underestimation might be improved by adding training data with a greater AGB in further study. The present study indicates that this CNN-based estimation method is highly versatile and could be a practical tool for monitoring crop AGB in diverse cultivars.

ARTICLE HISTORY
Received 17 November 2022
Revised 19 March 2023
Accepted 14 April 2023

KEYWORDS
Above-ground biomass; Biomass estimation; Convolutional neural network; Digital image; Rice; World rice core collection

Introduction

The global food demand for 2050 is projected to increase by 35–56% compared to 2010 (van Dijk et al., 2021). To meet the rising food demand, crop production per unit area needs to be enhanced through improvements in field management and genetic potential (Cooper et al., 2021). Above-ground biomass (AGB), which is defined as the above-ground dry weight per unit area, is one of the most important indicators for determining crop productivity (Long et al., 2006). Crop AGB increases with crop growth and is greatly affected by the cultivar, growth environment, and field management (de Bossoreille de Ribou et al., 2013). Conventionally, AGB has been evaluated through destructive sampling of crops, which requires a large area of land and considerable effort. The availability of AGB data with sufficient quality and quantity has been limited in various situations, such as farmers' fields in developing countries or the screening of high-yielding cultivars in breeding programs. Insufficient access to AGB data has been a potential barrier to achieving sustainable and increased crop production.

To monitor crop AGB, several non-destructive estimation methods have been developed. In previous studies, the AGB of various crops was successfully estimated by regression analysis using vegetation indices (VIs). VIs are generally calculated from optical information gathered using special sensors, such as hyperspectral and multispectral sensors mounted on unmanned aerial vehicles (UAV) or satellites (Alebele et al., 2020; Y. Wang et al., 2019). Recently, the estimation accuracy of VI-based methods has improved with the addition of input variables, such as textural, structural, and meteorological features (Q. Jiang et al., 2019; Xu et al., 2022), and the introduction of improved feature extraction methods,

CONTACT Yu Tanaka tanaka.yu.2s@kyoto-u.ac.jp Graduate School of Environmental, Life, Natural Science and Technology, Okayama University, Okayama, Japan

AUTHOR NOTES
The date of submission: Feb. 13, 2023.
Supplemental data for this article can be accessed online at https://doi.org/10.1080/1343943X.2023.2210767.

including machine-learning techniques (Jimenez-Sierra et al., 2021; L. Wang et al., 2016). However, these VI-based methods are limited in terms of versatility and cost. First, the relationship between crop AGB and VIs can vary depending on crop species, cultivars, canopy architecture, and growth environment (Aparicio et al., 2002; Hatfield & Prueger, 2010; ten Harkel et al., 2019). Second, special knowledge and expensive sensors are required to obtain VIs (Ma et al., 2019). Such low versatility and high cost have been major obstacles to the practical and widespread use of VI-based estimations by crop producers and scientists. Although there are also Red Green Blue (RGB) image-based VIs, which can be taken with low-cost and easy-to-use devices, including digital cameras, the estimation accuracy of RGB image-based VIs tends to be lower than that of VIs from hyperspectral and multispectral sensors (T. Wang et al., 2021). Therefore, highly versatile and low-cost methods for estimating crop AGB should be explored.

Deep learning (DL) technology has been developing rapidly. Among the different approaches in DL, convolutional neural network (CNN) has achieved state-of-the-art results in RGB image-based recognition tasks (Mochida et al., 2019). A CNN consists of several layers, including convolutional and pooling layers. In convolutional layers, feature maps are extracted from high-dimensional data, such as RGB images, through convolutional calculations. In the pooling layers, feature maps are compressed while retaining the important features. By combining these layers, the final output can be calculated based on the features extracted from the input RGB images. In the training process of the CNN, the parameters in each layer were gradually modified based on the error calculated from the difference between the estimated value and the ground truth. By repetitive modification of the parameters, the CNN model can extract important features from RGB images and calculate accurate outputs. The trained CNN model shows higher accuracy and versatility than other feature extraction methods for image analyses in the agricultural domain (Kamilaris & Prenafeta-Boldú, 2017). Therefore, CNN is expected to accelerate plant phenotyping (Y. Jiang & Li, 2020).

Owing to the high accuracy and versatility of the CNN model, many agronomical studies have already applied CNN not only to classification tasks, such as disease detection (Fuentes et al., 2017) and weed segmentation (Milioto et al., 2018) but also to regression tasks, such as yield estimation (Yang et al., 2019) and leaf-area-index (LAI) estimation (Yamaguchi et al., 2020). There are also many studies that utilized CNN to estimate crop AGB from RGB images and showed high estimation accuracy (Han et al., 2022; Ma et al., 2019; Schreiber et al., 2022). However, previous study used only a few cultivars to establish a CNN-based estimation model for crop AGB. Since different image quality caused by diverse canopy architecture can largely affect the accuracy of the model, the versatility of CNN-based AGB estimation for diverse cultivars having different canopy architectures should be investigated.

In the present study, we focused on rice, which is an important cereal crop and has the third-highest production quantity among cereal crops (FAOSTAT, 2020). We used a rice diversity panel, World Rice Core Collection (WRC) with some reference cultivars in the present study. The WRC consists of 69 cultivars. These cultivars were selected from approximately 30 thousand accessions and cover over 90% of genetic diversity (Kojima et al., 2005). Considering that genetic factors are responsible for the diversity of canopy architecture in rice (Y. Wang & Li, 2005; Zhao et al., 2011), the cultivars in the WRC were expected to have diverse canopy architectures. These cultivars are considered to be an ideal material for this research. We constructed a large-scale database of the RGB images of 59 rice cultivars and their corresponding AGB. We then established a CNN model to estimate rice AGB from RGB images by training the CNN with the established dataset. After establishing the model, we evaluated its estimation accuracy for the test and independent prediction datasets to confirm its versatility.

Materials and methods

Cultivation condition

The field experiment was conducted in 2019 and 2020 across two locations: an experimental paddy field in the Graduate School of Agriculture, Kyoto University, Japan (hereinafter called 'Kyoto') (35.2N, 135.47E); and an experimental paddy field in the Field Museum Honmachi, Tokyo University of Agriculture and Technology, Honmachi, Fuchu-shi, Tokyo (hereinafter called 'Tokyo') (35.41N, 139.29E). In total, 59 cultivars were grown. In 2019, four cultivars were grown in Kyoto. One of these was the temperate subspecies japonica (Koshihikari), while the other three cultivars were indica (Kasalath, Takanari, and Hokuriku 193). In 2019, three cultivars were grown in Tokyo. Two of them were temperate japonica (Koshihikari and Akitakomachi), and one cultivar was indica (Takanari). In 2020, 54 and 26 cultivars were cultivated in Kyoto and Tokyo, respectively, and 52 of the 54 and 21 of the 26 cultivars were selected from WRC. Details of the cultivars are presented in Table S1. All the fields were sufficiently irrigated during the growing season. All the plants were transplanted. In Kyoto, the transplanting dates were 17 May 2019, and 15 May 2020. In Tokyo, the transplanting dates were May 22, June 6, and 19 June 2019, and May 20, June 3, and 17 June 2020. One or three rice plants were transplanted per hill. Planting density ranged from 11.1 to 25.0 hills m^{-2}. Total nitrogen fertilizer application ranged from 0 to 18 g m^{-2}. The detailed cultivation conditions are listed in Supplementary Table S4.

The seeds of WRC were provided by the Genebank at National Agriculture and Food Research Organization, Japan, with the standard material transfer agreement. All the field experiments in this study complied with relevant institutional, national, and international guidelines and legislation.

Construction of database with RGB images and corresponding AGB

RGB images of the rice canopy and its corresponding AGB were manually collected. The procedure for the database

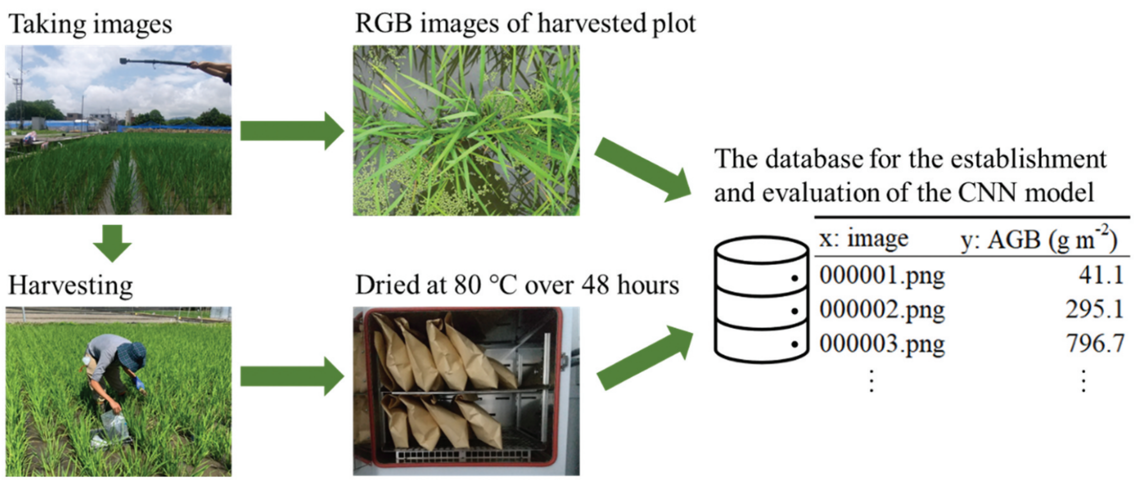

Figure 1. Procedure for database construction. We took RGB images of canopy at harvested plots using a commercial digital camera. We then harvested two successive rice plants and dried it at 80°C for 48 hours to determine the AGB.

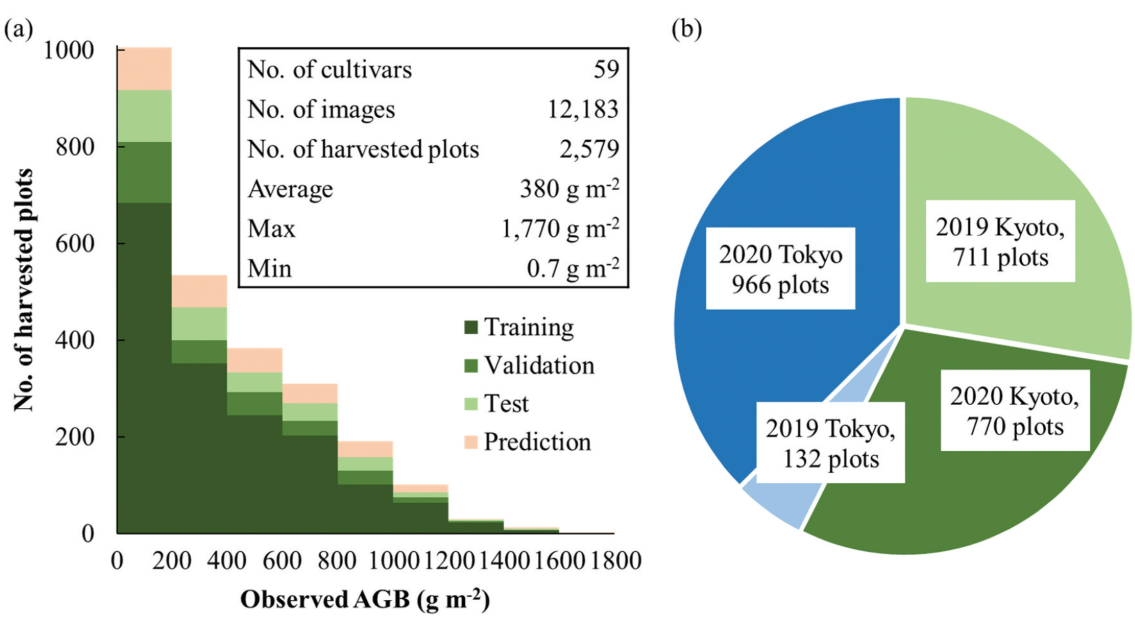

Figure 2. Summary of the collected data. (a) Bar plot showing the distribution of the observed above-ground biomass (AGB) in each dataset; (b) Pie-chart of the dataset composition of each location and year with the number of plots in each location and year.

construction is shown in Figure 1. Across all experiments, data collection was conducted 97 times from 2 weeks after transplanting to approximately 1 week after heading. Two successive hills were set as one harvesting plot. In total, 12183 images were taken from 2,579 harvested plots. Figure 2 and Supplementary Table 5 summarize the database.

At each harvesting plot, RGB images were taken to cover 0.12 m^{-2}. Two target rice plants were located in the right and left halves of the image, respectively. All images were taken vertically downward from approximately 1.5 m above the ground using an OLYMPUS TG-5 (Olympus, Tokyo, Japan) digital camera. Even when the plant height exceeded over 1.5 m, the way of taking images didn't change. In that case, the camera was inside the canopy. The optical zoom was set to 3×, which was identical to a focal length of 75 mm (35 m film equivalent). All images were taken at a 4000 × 3000 pixels spatial resolution, with flash always off, and stored in JPG file format. In Kyoto, four or five images were captured by moving the camera slightly for data augmentation. In 2020, at 62, 79, and 93 DAS, plant height and SPAD values were measured for all 54 cultivars in Kyoto. Each value was measured from five hills around the harvesting plot and was averaged. SPAD values were measured using a portable chlorophyll meter (SPAD-502, Minolta, Japan). The plants in the two successive hills at each harvesting plot where RGB images were taken were immediately harvested and dried at 80°C for 48 hours. Each dried sample was weighed to determine the AGB (g m^{-2}).

Construction of datasets for model establishment and prediction

All data were categorized into two parts: model establishment and prediction. Table S1 shows the detailed list of cultivars in each category. The model establishment category consisted of 28 cultivars grown for two years across two locations. The prediction category consisted of the other 31 cultivars grown in Kyoto in 2020. The model establishment category was further separated into the training, validation, and test datasets. The training dataset contained 7,911 images from 1,688 harvested plots and was used to determine the model parameters. The validation dataset contained 1,373 images from 293 plots and was used to verify the determined parameters. The test dataset contained 1,389 images from 296 plots and was used to verify the accuracy of the established model. The prediction category contained a dataset of 1,510 images from 302 plots and was designed to verify the accuracy of the established model, particularly for the independent dataset. Table 1 summarizes each dataset.

Images in all datasets were resized to 300 × 225 pixels with a bilinear algorithm, and used as inputs for the CNN model. The ground sample distance of the resized images was approximately 1.3 mm per pixels. For data augmentation, the images taken in Tokyo over two years were cropped to 296 × 222 pixels in four ways by moving the position of the cropping frame. The cropped images were resized to 300 × 225 pixels using a bilinear algorithm.

Establishment of the CNN model

The CNN structure developed in our previous study (Tanaka et al., 2021) for estimating rice grain yield was applied in the present study. In our previous study, an automated search for CNN structure in Neural Network Console software (Sony Network Communications Inc., Japan) was conducted to create diverse patterns of CNN structure. Then, the CNN structure which showed low computational cost and satisfactory high accuracy was chosen (Tanaka et al., 2021). This CNN structure also showed the high accuracy for estimating rice AGB in the preliminary analyses. The structure of the CNN is shown in Supplementary Figure . S1. The CNN structure had three branches, nine convolutional layers, and one fully connected layer. The CNN model was implemented using Python (version 3.6.8) with TensorFlow framework (version 2.1.0). The weights and biases of the network were initialized to a uniform distribution and zero, respectively, according to the defaults of the TensorFlow framework. The Adam algorithm was used as the optimizer. The loss function was defined by the

Table 1. Composition of the dataset category.

Category name	Location & Year	Dataset name	No. of cultivars	No. of images	No. of harvested plots
Model establishment	2019 Kyoto, 2019 Tokyo, 2020 Kyoto, 2020 Tokyo	Training		7,911	1,688
		Validation	28	1,373	293
		Test		1,389	296
Prediction	2020 Kyoto	Prediction	31	1,510	302
			59	12,183	2,579

RMSE. The number of epochs was set as 100. In all trials, the best parameters in the model were determined when the lowest validation loss was recorded. Learning rate decay was conducted by dropping the learning rate every 20 epochs. The learning rate for every 20 epochs was calculated by multiplying the initial learning rate by 0.8, 0.6, 0.4, and 0.2.

The hyperparameters were tuned by changing the batch size and initial learning rate. The optimal combination of batch size and initial learning rate was determined by changing both values. The batch size was changed to 4, 8, 16, 32, 64, 128, or 256. The initial learning rate was changed to 0.1, 0.01, 0.001, 0.0001, or 0.00001. The best combination of the batch size and initial learning rate was determined based on the estimation accuracy for the test dataset. The CNN model was trained using the best combination of the batch size and initial learning rate. The trained model was used to estimate rice AGB.

AGB estimation with the established model

All RGB images of the validation, test, and prediction datasets were input into the established model to estimate rice AGB. Four or five points of estimated AGB from the same harvested plots were obtained from the augmented images. The values were averaged to evaluate the estimation accuracy for each harvested plot. RMSE, rRMSE, and R^2 were calculated as indicators of estimation accuracy. RMSE and rRMSE were defined as shown in Eq. 1 and Eq. 2:

$$RMSE = \sqrt{\frac{1}{n}\sum_{i=1}^{n}(y_i - \hat{y}_i)^2} \tag{1}$$

$$rRMSE = \frac{1}{\bar{y}}\sqrt{\frac{1}{n}\sum_{i=1}^{n}(y_i - \hat{y}_i)^2} \tag{2}$$

where n is the number of harvested plots, y_i and $\hat{y}_i$ are the individual estimated and observed AGB, respectively, and $\bar{y}$ is the average of the observed AGB. Linear regression analysis was applied to show the estimation tendency.

Segmented linear regression analysis (Eq. (3)) was additionally performed on the results of the prediction dataset because it was clear that the estimated AGB saturated in greater AGB. The segmented linear regression analysis was used to determine the applicable range of the model and to discuss the results separately within and outside the range.

$$y = ax + b + (-ax + ac) \cdot I_{(x-c)} \tag{3}$$

where y is the estimated AGB, parameters a and b are constants, x is the measured AGB, c is the junction point of the segments, and I is a step function defined as follows:

$$I_{(x-c)} = \begin{cases} 0(x \leq c) \\ 1(x > c) \end{cases}$$

(Eq. 4)The coefficients a, b, and c were determined by minimizing the sum of squared residuals between the estimated AGB (as the true y value) and predicted values from the regression line with the Solver Add-in in Microsoft Excel (Microsoft, Redmond, WA, USA).

The rRMSE of each cultivar in the prediction dataset was calculated using the AGB data less than the junction point to reveal differences in estimation accuracy among cultivars. The time course of plant height and SPAD values for 31 cultivars of the prediction dataset were plotted to explore the visual characteristics of the cultivar with a significantly high rRMSE. The correlations between the rRMSE of the 31 cultivars calculated in this study and several traits measured in the previous study (Kojima et al., 2005) were investigated. All analyses in this study were conducted using Microsoft Excel (Microsoft, Redmond, WA, USA) and Python version 3.6.8 (http://www.python.org) with TensorFlow framework version 2.1.0 (https://www.tensorflow.org). The code for implementing the established model is available at https://github.com/KotaNakajima/rice_biomass_CNN.git.

Results

Construction of database and the CNN model for AGB estimation

Across two years at two locations, 59 cultivars mainly from WRC were cultivated and 12,183 images were taken from 2,579 harvested plots (Figure 2a). Of the 2,579 harvested plots, 58% and 42% of the data were collected in Kyoto and Tokyo, respectively (Figure 2b). The observed AGB ranged from 0.7 g m^{-2} to 1,770 g m^{-2}, with an average of 3.80 g m^{-2} (Figure 2a). The frequency of the observed AGB data decreased as the observed AGB value increased. The observed AGB value was higher than 1,000 g m^{-2} for only 5.9% of the entire data.

We applied the RGB-based CNN structure with nine convolutional layers and three branches (Supplementary Figure . S1), reported previously for estimating rice yield (Tanaka et al., 2021). To determine the hyperparameters for obtaining the best accuracy, we tuned the hyperparameters by a grid search. We tested the combination of batch size and initial learning rate from 4 to 256 and 0.1 to 0.00001, respectively, with ten replicated trials. We

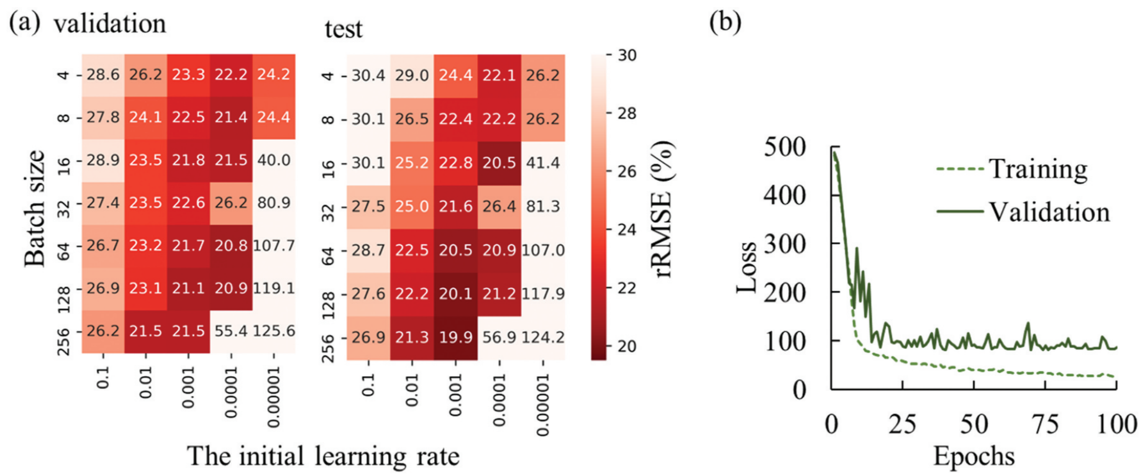

Figure 3. Establishment of a convolutional neural network (CNN) model for AGB estimation. (a) the loss value for validation and test datasets at different batch sizes and initial learning rates; (b) the learning curve of the determined model.

found that the combination of a batch size of 256 and an initial learning rate of 0.001 resulted in the lowest relative root mean square error (rRMSE) for the test dataset (Figure. 3a). The CNN model was trained using the best combination of batch size and initial learning rate. Figure. 3b shows the learning curve of the model. The loss value of the training dataset decreased smoothly. The loss value for the validation dataset decreased smoothly at first and then reached a plateau. The lowest validation loss was recorded at the 70th epoch, and the model with parameters determined at the 70th epoch was used for all subsequent analyses.

Evaluation of the established CNN model

Using the rice RGB images as input, the CNN model could estimate the rice AGB of the validation and test datasets, which ranged from approximately 0 to 1,500 g m^{-2} (Figure 4). here was no clarity regarding the overestimation or underestimation of data across different cultivars, growth stages, locations, and years. The model estimated the AGB of 28 cultivars included in the validation dataset with root mean square error (RMSE) of 77 g m^{-2}, rRMSE of 21.0%, and coefficient of determination (R^2) of 0.94 (Figure 4a). The slope and intercept of the regression line were 0.96 and 4.46, respectively. The model also estimated the AGB from the test dataset with RMSE of 72 g m^{-2}, rRMSE of 18.6%, and R^2 of 0.95 (Figure 4b). The slope and intercept of the regression line were 0.95 and 2.27, respectively.

For the 31 cultivars in the prediction dataset that were not included in the model establishment category, the AGB estimated by the model showed a clear correlation with the observed AGB, but a significant

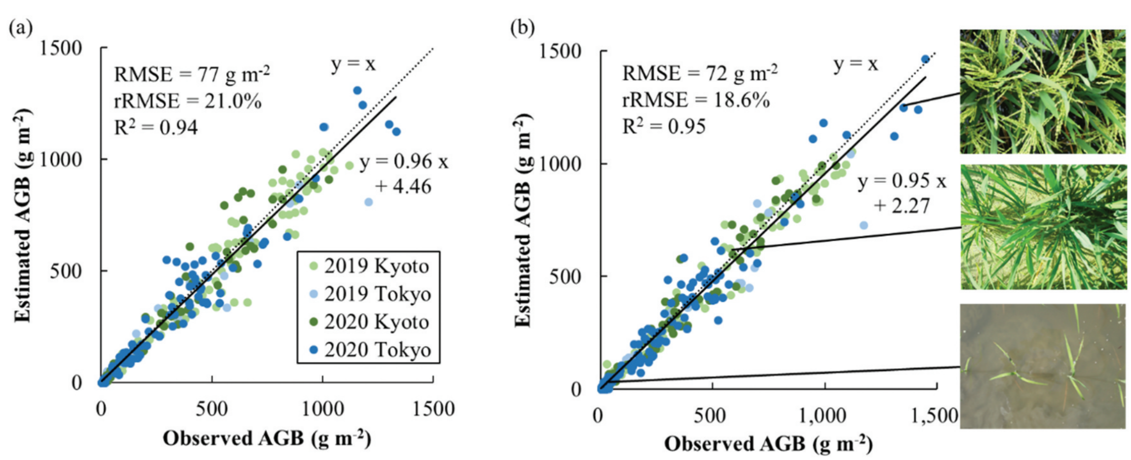

Figure 4. Correlations between observed AGB and estimated AGB at each harvested plot. (a) Estimated AGB of the validation dataset; (b) Estimated AGB of the test dataset. The three RGB images in Figure 4(b) are examples of input RGB images used for the estimation. The dotted line represents the 1:1 line, and the solid line represents the fitted line.

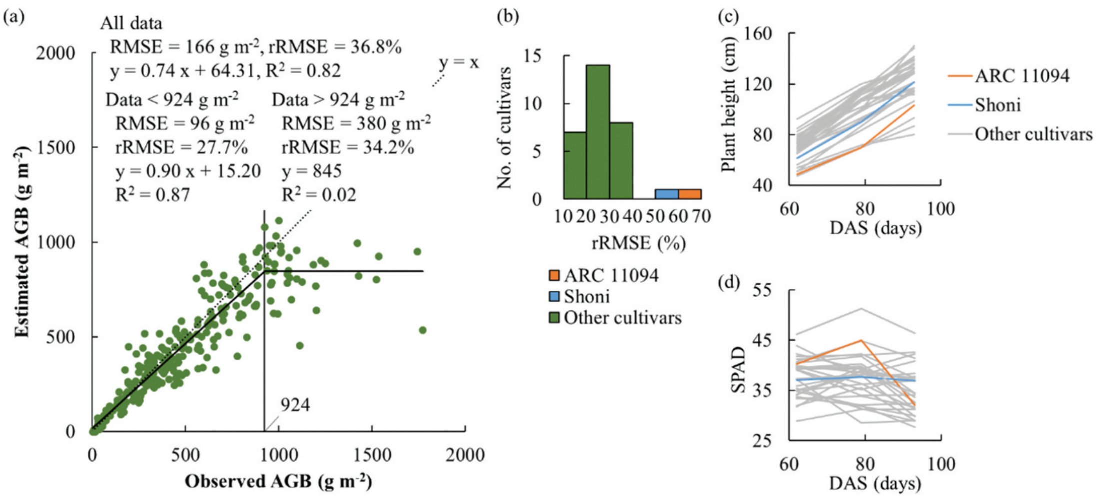

Figure 5. Estimation result on the prediction dataset: (a) Correlations between observed AGB and estimated AGB of the prediction dataset at each harvested plot. The dotted line represents the 1:1 line, and the solid line represents the fitted segmented regression line; (b) the bar plot depicting the distribution of the calculated rRMSE of each cultivar in the prediction dataset; (c) the time-course change of plant height of 31 cultivars in the prediction dataset; (d) the time-course change of the SPAD value of 31 cultivars in the prediction dataset.

underestimation was observed with higher values of AGB (Figure 5a). The model estimated the AGB from the prediction dataset with RMSE of 166 g m^{-2}, rRMSE of 36.8%, and R^2 of 0.82, respectively. When segmented regression was applied, it was revealed that the CNN model could not estimate AGB well when the observed AGB was greater than 924 g m^{-2} (R^2 of 0.02). On the other hand, it successfully estimated AGB when the observed AGB was lesser than 924 g m^{-2} with RMSE of 96 g m^{-2}, rRMSE of 27.7% and R^2 of 0.87 (Figure 5a). The slope and intercept of the segmented regression line for this range was 0.90 and 15.20, respectively.

A significant difference was observed in the rRMSE calculated for each cultivar in the prediction dataset (Table S2). For observed AGB lower than 924 g m^{-2}, the rRMSE of each cultivar ranged from 14.5% (for Puluik Arang) to 66.1% (for ARC 11,094), with an average of 27.0% and a median of 24.7% (Figure 5b and Table S3). The rRMSE of 29 cultivars was lower than 37.6%, whereas the rRMSE of two cultivars, ARC 11,094 and Shoni, were outliers. To elucidate the visual characteristics of these two cultivars, the plant height and soil-plant analysis development (SPAD) value (an indicator of the chlorophyll content in leaves) of 31 cultivars in the prediction dataset were measured 62, 79, and 93 days after sowing (DAS). Figures 5c and 5d show the time course of plant height and SPAD value of the 31 cultivars. ARC 11,094 showed one of the lowest plant heights. The SPAD values of ARC 11,094 at 62 and 79 DAS were one of the highest among the 31 cultivars, while it decreased drastically at 93 DAS. Shoni showed a plant height lower than the average. The SPAD values of Shoni were relatively stable throughout all measurements and were near the average value for the 31 cultivars. Table S6 and Supplementary Figure . S1 shows the correlation between rRMSE of the 31 cultivars and each of several traits measured in the previous study (Kojima et al., 2005). The traits that showed the highest correlation (−0.3) and second highest correlation (−0.27) with rRMSE were panicle length and culm length, respectively.

Discussion

Most non-destructive estimations of crop AGB are based on optical information, such as VIs, taken from UAVs or satellites (Chao et al., 2019). The AGB of various crop species, including rice, has been successfully estimated using VI-based methods. However, these methods have limitations in terms of their versatility and cost. First, the established model tends to be case-sensitive because the relationship between VIs and AGB varies depending on crop species, cultivars, and growth environments (Aparicio et al., 2002; Hatfield & Prueger, 2010; ten Harkel et al., 2019). Second, specialized knowledge and expensive devices, such as multispectral or hyperspectral sensors and UAVs, are required to obtain VIs (Ma et al., 2019). The insufficient versatility and high cost of most previous AGB estimation methods are barriers to the full utilization of these technologies by crop producers and scientists.

In the present study, we established and evaluated a CNN-based estimation model for rice AGB using RGB images. Regarding the AGB range, the model was applicable up to approximately 1,500 g m^{-2} and 924 g m^{-2} for the test and prediction datasets, respectively. This indicates that our model is applicable until the heading stage in many cultivars. Regarding the estimation accuracy, the model estimated rice AGB with R^2 of 0.95 and 0.82 for the test and prediction datasets, respectively. For the prediction dataset, R^2 was 0.87 when the observed AGB was lesser than 924 g m^{-2}. These estimation accuracies are comparable to or even higher than those reported in previous VI-based studies (Alebele et al., 2020; Jimenez-Sierra et al., 2021; Q. Jiang et al., 2019; Xu et al., 2022; Y. Wang et al., 2019).

While there are several studies on estimating crop AGB using CNN (Han et al., 2022; Ma et al., 2019; Schreiber et al., 2022), these studies used only a few cultivars. Therefore, little is known about the versatility of the CNN-based estimation method for different image quality caused by diverse cultivars having various canopy architectures. Our model was applicable not only to the 28 cultivars in the test dataset but also to the 31 independent cultivars in the prediction dataset. These 59 diverse cultivars were mainly from WRC which expected to have diverse plant architecture. Notably, the cultivars in the prediction dataset were not included in any other dataset. These results indicate that the CNN model has sufficient versatility to accommodate diverse image quality and the plant architectures of different cultivars.

In addition, considering that the data in the test dataset were obtained at two locations, our results imply that the CNN-based estimation for crop AGB also has the potential of versatility for the environment. In terms of cost, our CNN model only requires RGB images, which can be obtained using commercial digital cameras or smartphones. In addition, our CNN structure is much smaller than the typical CNN models for image recognition such as VGG16 and ResNet (He et al., 2016; Simonyan & Zisserman, 2014). These features can empower crop producers and scientists by enabling them to perform on-site estimation of rice AGB for diverse cultivars and environments.

However, the established model presents several challenges. First, for the prediction dataset, which included 31 independent cultivars, the estimated AGB saturated when the observed AGB was greater than 924 g m^{-2}. In the training dataset, only 7.7% of data showed AGB greater than 924 g m^{-2}. Generally, the accuracy and versatility of CNN models increase as the model is trained with more data (Marcus, 2018; Sun et al., 2017). Thus, further studies should include more data with a greater AGB in the training dataset. Second, the rRMSE of each cultivar in the prediction dataset was significantly different. The rRMSE values of the ARC 11,094 and Shoni cultivars were much greater than those of the other cultivars. The plant height and SPAD values of the 31 cultivars in the prediction dataset were measured, and the plant height of ARC 11,094 and Shoni tended to be the lowest among the 31 cultivars. This may imply that the estimation accuracy of the model is significantly worse for cultivars with low plant heights. Among the correlations between the rRMSE calculated in this study and the traits measured in the previous study, the highest correlation coefficient was −0.3 and the relationships were not clear (Table S6, Supplementary Figure . S1). The effects of other factors such as tiller number and leaf angle should be investigated. Third, the shooting range of the images was considered too small to monitor rice AGB across the field. Each image covered two successive hills, which were approximately 0.12 m^{-2}. It would be labor-intensive to apply this CNN-based method to large farmland. The shooting range of the images should be expanded in further study. Fourth, the model's versatility for the diversity of growth conditions among rice production fields has not been sufficiently verified. In the present study, all data were collected over two years in two experimental fields under proper management. The planting densities of all cultivars were almost the same. There were no data indicating that the plants were affected by the lodging, lack of hills, weeds, diseases, or abiotic stresses. It is well known that crop AGB is strongly affected not only by cultivars but also by growth conditions, including environmental factors and field management practices (Cossani et al., 2009). Therefore, future studies should establish a model with more diverse growth condition data.

In conclusion, we investigated the versatility of CNN-based AGB estimation for diverse cultivars having different canopy architectures. We established and evaluated the CNN model using RGB images with 59 diverse cultivars, which were mainly from WRC. The established model accurately estimated the rice AGB of 28 cultivars in the test dataset. It is noteworthy that the model was also applicable to 31 cultivars that were not included in the model establishment. The results emphasize the high versatility of the CNN model for diverse cultivars having various plant architectures. In addition, the CNN model only requires RGB images, which can be easily obtained using a low-cost device. Our results will be the basis to enable crop producers and scientists to monitor the AGB of diverse rice cultivars on-site and at a reasonable cost. Such on-site monitoring will contribute to enhancing rice productivity by allowing better field management, enabling the crop to achieve its full genetic potential.

Acknowledgments

We thank Dr. Yu Iwahashi at Kyoto University for the support of the field experiment. We are also appreciated to National Agriculture and Food Research Organization, Japan, for providing the seeds of WRC.

Disclosure statement

No potential conflict of interest was reported by the authors.

Funding

This work was supported in part by the Japan Science and Technology Agency PRESTO grant number JPMJPR16Q5 (to Y. T.) and the Japan Society for the Promotion of Science (JSPS) KAKENHI grant number 20H02968 (to Y.T. and K.K.) and 21K19104 (to Y.T.).

ORCID

Yu Tanaka http://orcid.org/0000-0003-2106-4217
Keisuke Katsura http://orcid.org/0000-0002-8856-8500

Data availability statement

The data supporting the findings of this study are available from the authors upon reasonable request (https://github.com/KotaNakajima/rice_biomass_CNN.git).

References

Alebele, Y., Zhang, X., Wang, W., Yang, G., Yao, X., Zheng, H., Zhu, Y., Cao, W., & Cheng, T. (2020). Estimation of canopy biomass components in paddy rice from combined optical and SAR data using multi-target gaussian regressor stacking. *Remote Sensing*, *12*(16), 2564. https://doi.org/10.3390/rs12162564

Aparicio, N., Villegas, D., Araus, J. L., Casadesús, J., & Royo, C. (2002). Relationship between growth traits and spectral vegetation indices in durum wheat. *Crop Science*, *42*(5), 1547–1555. https://doi.org/10.2135/cropsci2002.1547

Chao, Z. H., Liu, N., Zhang, P. D., Ying, T. Y., & Song, K. H. (2019). Estimation methods developing with remote sensing information for energy crop biomass: A comparative review. *Biomass & Bioenergy*, *122*, 414–425. https://doi.org/10.1016/j.biombioe.2019.02.002

Cooper, M., Voss-Fels, K. P., Messina, C. D., Tang, T., & Hammer, G. L. (2021). Tackling G × E × M interactions to close on-farm yield-gaps: Creating novel pathways for crop improvement by predicting contributions of genetics and management to crop productivity. *Theoretical and Applied Genetics*, *134*(6), 1625–1644. https://doi.org/10.1007/s00122-021-03812-3

Cossani, C. M., Slafer, G. A., & Savin, R. (2009). Yield and biomass in wheat and barley under a range of conditions in a Mediterranean site. *Field Crops Research*, *112*(2–3), 205–213. https://doi.org/10.1016/j.fcr.2009.03.003

de Bossoreille de Ribou, S., Douam, F., Hamant, O., Frohlich, M. W., & Negrutiu, I. (2013). Plant science and agricultural productivity: Why are we hitting the yield ceiling? *Plant Science*, *210*, 159–176. https://doi.org/10.1016/j.plantsci.2013.05.010

FAOSTAT http://faostat.fao.org. (2020).

Fuentes, A., Yoon, S., Kim, S., & Park, D. (2017). A robust deep-learning-based detector for real-time tomato plant diseases and pests recognition. *Sensors*, *17*(9), 2022. https://doi.org/10.3390/s17092022

Han, J., Shi, L., Yang, Q., Chen, Z., Yu, J., & Zha, Y. (2022). Rice yield estimation using a CNN-based image-driven data assimilation framework. *Field Crops Research*, *288*, 108693. https://doi.org/10.1016/j.fcr.2022.108693

Hatfield, J. L., & Prueger, J. H. (2010). Value of using different vegetative indices to quantify agricultural crop characteristics at different growth stages under varying management practices. *Remote Sensing*, *2*(2), 562–578. https://doi.org/10.3390/rs2020562

He, K., Zhang, X., Ren, S., & Sun, J. (2016). Deep residual learning for image recognition. *2016 IEEE Conference on Computer Vision and Pattern Recognition (CVPR)*, Las Vegas, NV, USA (pp. 770–778).

Jiang, Q., Fang, S., Peng, Y., Gong, Y., Zhu, R., Wu, X., Ma, Y., Duan, B., & Liu, J. (2019). UAV-based biomass estimation for rice-combining spectral, TIN-based structural and meteorological features. *Remote Sensing*, *11*(7), 890. https://doi.org/10.3390/rs11070890

Jiang, Y., & Li, C. (2020). Convolutional neural networks for image-based high-throughput plant phenotyping: A review. *Plant Phenomics*, *2020*, 1–22. https://doi.org/10.34133/2020/4152816

Jimenez-Sierra, D. A., Correa, E. S., Benítez-Restrepo, H. D., Calderon, F. C., Mondragon, I. F., & Colorado, J. D. (2021). Novel feature-extraction methods for the estimation of above-ground biomass in rice crops. *Sensors*, *21*(13), 4369. https://doi.org/10.3390/s21134369

Kamilaris, A., & Prenafeta-Boldú, F. X. (2017). A review of the use of convolutional neural networks in agriculture. *The Journal of Agricultural Science*, *156*(3), 312–322. https://doi.org/10.1017/S0021859618000436

Kojima, Y., Ebana, K., Fukuoka, S., Nagamine, T., & Kawase, M. (2005). Development of an RFLP-based rice diversity research set of germplasm. *Breeding Science*, *55*(4), 431–440. https://doi.org/10.1270/jsbbs.55.431

Long, S. P., Zhu, X. -G., Naidu, S. L., & Ort, D. R. (2006). Can improvement in photosynthesis increase crop yields? *Plant, Cell & Environment*, *29*(3), 315–330. https://doi.org/10.1111/j.1365-3040.2005.01493.x

Ma, J., Li, Y., Chen, Y., Du, K., Zheng, F., Zhang, L., & Sun, Z. (2019). Estimating above ground biomass of winter wheat at early growth stages using digital images and deep convolutional neural network. *European Journal of Agronomy*, *103*, 117–129. https://doi.org/10.1016/j.eja.2018.12.004

Marcus, G. (2018). Deep learning: A critical appraisal. *Arxiv Preprint*, *arXiv:1801*(00631), 1–27. https://doi.org/10.48550/arXiv.1801.00631

Milioto, A., Lottes, P., & Stachniss, C. (2018). Real-time semantic segmentation of crop and weed for precision agriculture robots leveraging background knowledge in CNNs. *2018 IEEE International Conference on Robotics and Automation (ICRA)*, Brisbane, Australia, (pp. 2229–2235).

Mochida, K., Koda, S., Inoue, K., Hirayama, T., Tanaka, S., Nishii, R., & Melgani, F. (2019). Computer vision-based phenotyping for improvement of plant productivity: A machine learning perspective. *GigaScience*, *8*(1), giy153. https://doi.org/10.1093/gigascience/giy153

Schreiber, L. V., Atkinson Amorim, J. G., Guimarães, L., Motta Matos, D., Maciel da Costa, C., & Parraga, A. (2022). Above-ground biomass wheat estimation: Deep learning with UAV-based RGB images. *Applied Artificial Intelligence*, *36*(1). https://doi.org/10.1080/08839514.2022.2055392

Simonyan, K., & Zisserman, A. (2014). Very deep convolutional networks for large-scale image recognition. *ArXiv Preprint, arXiv:1409*(1556), 1–14. https://doi.org/10.48550/arXiv.1409.1556

Sun, C., Shrivastava, A., Singh, S., & Gupta, A. (2017). Revisiting unreasonable effectiveness of data in deep learning era. *2017 IEEE International Conference on Computer Vision (ICCV)*, Venice, Italy (pp. 843–852).

Tanaka, Y. (2021). Deep learning-based estimation of rice yield using RGB image. *PREPRINT (Version 1) is Available at Research Square*. https://doi.org/10.21203/rs.3.rs1026695/v1

ten Harkel, J., Bartholomeus, H., & Kooistra, L. (2019). Biomass and crop height estimation of different crops using UAV-based lidar. *Remote Sensing*, *12*(1), 17. https://doi.org/10.3390/rs12010017

van Dijk, M., Morley, T., Rau, M. L., & Saghai, Y. (2021). A meta-analysis of projected global food demand and population at risk of hunger for the period 2010–2050. *Nature Food*, *2*(7), 494–501. https://doi.org/10.1038/s43016-021-00322-9

Wang, Y., & Li, J. (2005). The plant architecture of rice (*Oryza sativa*) *Plant Mol. Plant Molecular Biology*, *59*(1), 75–84. https://doi.org/10.1007/s11103-004-4038-x

Wang, T., Liu, Y., Wang, M., Fan, Q., Tian, H., Qiao, X., & Li, Y. (2021). Applications of UAS in crop biomass monitoring: A review. *Frontiers in Plant Science*, *12*, 616689. https://doi.org/10.3389/fpls.2021.616689

Wang, Y., Zhang, K., Tang, C., Cao, Q., Tian, Y., Zhu, Y., Cao, W., & Liu, X. (2019). Estimation of rice growth parameters based on linear mixed-effect model using multispectral images from fixed-wing unmanned aerial vehicles. *Remote Sensing*, *11*(11), 1371. https://doi.org/10.3390/rs11111371

Wang, L., Zhou, X., Guo, Z., Dong, W., & Guo, W. (2016). Estimation of biomass in wheat using random forest regression algorithm and remote sensing data. *The Crop Journal*, *4*(3), 212–219. https://doi.org/10.1016/j.cj.2016.01.008

Xu, L., Zhou, L., Meng, R., Zhao, F., Lv, Z., Xu, B., Zeng, L., Yu, X., & Peng, S. (2022). An improved approach to estimate ratoon rice above-ground biomass by integrating UAV-based spectral, textural and structural features. *Precision Agriculture*, *23*(4), 1276–1301. https://doi.org/10.1007/s11119-022-09884-5

Yamaguchi, T., Tanaka, Y., Imachi, Y., Yamashita, M., & Katsura, K. (2020). Feasibility of combining deep learning and RGB images obtained by unmanned aerial vehicle for leaf area index estimation in rice. *Remote Sensing*, *13*(1), 84. https://doi.org/10.3390/rs13010084

Yang, Q., Shi, L., Han, J., Zha, Y., & Zhu, P. (2019). Deep convolutional neural networks for rice grain yield estimation at the ripening stage using UAV-based remotely sensed images. *Field Crops Research*, *235*, 142–153. https://doi.org/10.1016/j.fcr.2019.02.022

Zhao, K., Tung, C. -W., Eizenga, G. C., Wright, M. H., Ali, M. L., Price, A. H., Norton, G. J., Islam, M. R., Reynolds, A., Mezey, J., McClung, A. M., Bustamante, C. D., & McCouch, S. R. (2011). Genome-wide association mapping reveals a rich genetic architecture of complex traits in *Oryza sativa*. *Nature Communications*, *2*(1), 467. https://doi.org/10.1038/ncomms1467